

PACS numbers: 42.62.Be; 42.25.Ja; 42.25.Lc; 87.64.kv
DOI: 10.1070/QE2014v044n08ABEH015295

Mueller-matrix mapping of optically anisotropic fluorophores of biological tissues in the diagnosis of cancer

Yu.A. Ushenko, M.I. Sidor, G.B. Bodnar, G.D. Koval'

Abstract. **We report the results of studying the polarisation manifestations of laser autofluorescence of optically anisotropic structures in biological tissues. A Mueller-matrix model is proposed to describe their complex anisotropy (linear and circular birefringence, linear and circular dichroism). The relationship is established between the mechanisms of optical anisotropy and polarisation manifestations of laser autofluorescence of histological sections of rectal tissue biopsy in different spectral regions. The ranges of changes in the statistical moments of the 1st-to-4th orders, which describe the distribution of the azimuth-invariant elements of Mueller matrices of rectal tissue autofluorescence, are found. Effectiveness of laser autofluorescence polarimetry is determined and the histological sections of biopsy of benign (polyp) and malignant (adenocarcinoma) tumours of the rectal wall are differentiated for the first time.**

Keywords: *autofluorescence, polarisation, birefringence, optical anisotropy, Mueller matrix, statistical moments, diagnostics.*

1. Introduction

Biological tissues represent structurally inhomogeneous optically anisotropic absorbing media. The description of the interaction of polarised light with such a complex system requires a more general approximation based on the use of the Mueller-matrix formalism. Currently, the biological and medical research relies on a variety of practical techniques involving the measurement and analysis of Mueller matrices of samples in question [1–10].

An independent branch, i.e., laser polarimetry, has emerged in matrix optics over the last 10–15 years [11]. Laser polarimetry makes it possible to establish the diagnostic relationship between a set of statistical moments of the 1st-to-4th orders [11, 12], which characterise the distribution of the Mueller-matrix elements, and linear birefringence in human tissues. Such an approach allows diagnosing cancer of skin dermis, connective and epithelial tissues of the female reproductive tract, etc. [11–13]. The main disadvantage of this diagnostic method is low accuracy caused by the azimuth dependence of the majority of the Mueller-matrix elements.

Yu.A. Ushenko, M.I. Sidor Yuriy Fedkovych Chernivtsi National University, ul. Kotsyubinskogo 2, 58012 Chernivtsi, Ukraine; e-mail: yuriyu@gmail.com;
G.B. Bodnar, G.D. Koval' Bukovinian State Medical University, Teatral'naya pl. 3, 58000 Chernivtsi, Ukraine

Received 14 August 2013; revision received 19 November 2013
Kvantovaya Elektronika **44** (8) 785–790 (2014)
Translated by I.A. Ulitkin

Simultaneously with the polarimetry techniques, alternative spectral methods based on the diagnostic application of fluorescence effects of protein molecules and their complexes are being intensely developed. The sensitivity obtained for the diagnosis of cancer in human organs is encouraging [14–20]. However, this optical technology is not accurate enough (specific) in terms of the differentiation of benign and malignant tumours of biological tissues. Since the publications devoted to the use of the Mueller-matrix formalism for the fluorescence analysis of ensembles of optically active protein molecules and their complexes are scarce [21, 22], the extension of the Mueller-matrix model to a more general case, i.e., fluorescence of birefringent networks of optically active complexes of biological tissues, and to the development of spectrally selective autofluorescence polarimetry on the basis of this method seems promising. This work is aimed at the realisation of these tasks for the differentiation of benign (polyp) and malignant (adenocarcinoma) tumours of rectal tissue.

2. Brief theory

In our work, we restricted ourselves to the spectrally selective ($\lambda = 0.63–0.65$ μm) case, i.e., luminescence of optically active porphyrins of biological tissue in the red region of the spectrum. Autofluorescence was excited with laser light having a wavelength of $\lambda = 0.405$ μm, which coincides with the absorption maximum of porphyrins [23].

Formation of laser polarisation fluorescence of biological tissue is based on the following model assumptions:

(i) on the mechanisms of optically anisotropic absorption (linear and circular dichroism) [24];

(ii) on the fluorescence of porphyrin molecules ('linear' oscillators) and liquid crystal networks formed by them ('elliptic' oscillators) [22];

(iii) on the mechanisms of phase anisotropy (linear and circular birefringence of fibrillar networks) that modulate the fluorescence [24].

The mentioned scenario can be described using the Mueller-matrix formalism.

Absorption. Fibrillar networks formed by optically active polypeptide protein chains are characterised by linear dichroism. Optical manifestations of this mechanism are described by the Mueller matrix [24]:

$$\{\Psi\} = \begin{Vmatrix} 1 & \varphi_{12} & \varphi_{13} & 0 \\ \varphi_{21} & \varphi_{22} & \varphi_{23} & 0 \\ \varphi_{31} & \varphi_{32} & \varphi_{33} & 0 \\ 0 & 0 & 0 & \varphi_{44} \end{Vmatrix}, \quad (1)$$

where

$$\varphi_{12} = \varphi_{21} = (1 - \Delta\tau)\cos 2\rho,$$

$$\varphi_{13} = \varphi_{31} = (1 - \Delta\tau)\sin 2\rho,$$

$$\varphi_{22} = (1 + \Delta\tau)\cos^2 2\rho + 2\sqrt{\Delta\tau}\sin^2 2\rho,$$

$$\varphi_{23} = \varphi_{32} = (1 - \Delta\tau)\sin 2\rho,$$

$$\varphi_{33} = (1 + \Delta\tau)\sin^2 2\rho + 2\sqrt{\Delta\tau}\cos^2 2\rho,$$

$$\varphi_{44} = 2\sqrt{\Delta\tau};$$

$\Delta\tau = \tau_x/\tau_y$; $\tau_x = \tau\cos\rho$, $\tau_y = \tau\sin\rho$; τ_x, τ_y are the absorption coefficients of linearly polarised orthogonal components of the amplitude of laser radiation; and ρ is the orientation of the optical axis of the fibril in the plane of the histological section of biological tissue.

The presence of a helical structure of protein molecules ensures circular dichroism, the optical manifestations of which are described by the matrix operator

$$\{\Phi\} = \begin{Vmatrix} 1 & 0 & 0 & \phi_{14} \\ 0 & \phi_{22} & 0 & 0 \\ 0 & 0 & \phi_{33} & 0 \\ \phi_{41} & 0 & 0 & 1 \end{Vmatrix}, \quad (2)$$

where

$$\phi_{22} = \phi_{33} = \frac{1 - \Delta g^2}{1 + \Delta g^2}, \quad \phi_{14} = \phi_{41} = \pm\frac{2\Delta g}{1 + \Delta g^2};$$

$\Delta g = (g_\otimes - g_\oplus)/(g_\otimes + g_\oplus)$; and $g_\otimes$ and $g_\oplus$ are the absorption coefficients of left- ($\otimes$) and right-hand ($\oplus$) circularly polarised components of the amplitude inducing the laser fluorescence.

Fluorescence. Polarisation manifestations of the fluorescence of porphyrins is characterised by the Mueller matrix for the ensembles of such molecules [22]:

$$\{F\} = \begin{Vmatrix} 1 & F_{12} & 0 & 0 \\ F_{21} & F_{22} & 0 & 0 \\ 0 & 0 & F_{33} & 0 \\ 0 & 0 & 0 & F_{44} \end{Vmatrix}. \quad (3)$$

Here,

$$F_{12} = F_{21} = -\frac{b\sin^2\vartheta}{a - b\sin^2\vartheta},$$

$$F_{22} = \frac{b(1 + \cos^2\vartheta)}{a - b\sin^2\vartheta},$$

$$F_{33} = \frac{2b\cos\vartheta}{a - b\sin^2\vartheta},$$

$$F_{44} = \frac{2c\cos\vartheta}{a - b\sin^2\vartheta};$$

ϑ is the scattering angle; and a and b are related constants defined for the system 'linear' oscillators in an isotropic medium by the relations

$$a = 0.5(1 + \langle\cos^2\varepsilon\rangle), \quad (4)$$

$$b = 0.25(3\langle\cos^2\varepsilon\rangle - 1), \quad (5)$$

where ε is the angle between the emission of a dipole and the polarisation azimuth of the illuminating beam. Zellweger [25] found two limiting values of $\langle\cos^2\varepsilon\rangle$: $\langle\cos^2\varepsilon\rangle = 3/5$ for a system of collinear dipoles and $\langle\cos^2\varepsilon\rangle = 1/3$ for a system of randomly oriented dipoles.

The parameter c is associated with optically activity of molecules [25]. Here, the emission of the ensembles (liquid crystal chains) of optically active molecules is considered as a set of 'elliptic oscillators'. In the limiting case, the specified parameter c reaches 5/16.

Phase modulation of porphyrin fluorescence. Fluorescence of linear and elliptic oscillators [relations (3)–(5)] formed by absorption mechanisms [relations (1) and (2)] propagates in the volume of optically anisotropic biological tissue. As a result, the fluorescence undergoes phase modulation, the basic mechanisms of which are the optical activity of amino acids and the thus formed polypeptide chains $\{\Omega\}$, as well as the birefringence of protein fibrillar networks $\{D\}$ [24]:

$$\{\Omega\} = \begin{Vmatrix} 1 & 0 & 0 & 0 \\ 0 & \omega_{22} & \omega_{23} & 0 \\ 0 & \omega_{32} & \omega_{33} & 0 \\ 0 & 0 & 0 & 1 \end{Vmatrix}, \quad (6)$$

$$\{D\} = \begin{Vmatrix} 1 & 0 & 0 & 0 \\ 0 & d_{22} & d_{23} & d_{24} \\ 0 & d_{32} & d_{33} & d_{34} \\ 0 & d_{42} & d_{43} & d_{44} \end{Vmatrix}. \quad (7)$$

Here,

$$\omega_{22} = \omega_{33} = \cos 2\gamma,$$

$$\omega_{23} = -\omega_{32} = \sin 2\gamma;$$

$$d_{22} = \cos^2 2\rho + \sin^2 2\rho\cos\delta,$$

$$d_{23} = d_{32}\cos 2\rho\sin 2\rho(1 - \cos\delta),$$

$$d_{33} = \sin^2 2\rho + \cos^2 2\rho\cos\delta,$$

$$d_{24} = -d_{42} = \sin 2\rho\sin\delta,$$

$$d_{34} = -d_{43} = \cos 2\rho\sin\delta,$$

$$d_{44} = \cos\delta;$$

γ is the angle of rotation of the polarisation plane of the fluorescence; and δ is the phase shift between the linearly polarised orthogonal components of the amplitude of the fluorescent.

Given all the above mechanisms of optically anisotropic absorption of laser light and phase modulation of the fluorescence of porphyrins, the resulting matrix of the fluorescence of biological tissue can be written in the form:

$$\{M\} = \{D\}\{\Omega\}\{F\}\{\Psi\}\{\Phi\} = \begin{Vmatrix} 1 & M_{12} & M_{13} & M_{14} \\ M_{21} & M_{22} & M_{23} & M_{24} \\ M_{31} & M_{32} & M_{33} & M_{34} \\ M_{41} & M_{42} & M_{43} & M_{44} \end{Vmatrix}. \quad (8)$$

Analysis of matrix (8) shows that the elements M_{ik} characterise the superposition of mechanisms of linear ($\Delta\tau$) and circular (Δg) dichroism as well as the fluorescence of linear

($F_{12,21,22,23}$) and elliptic (F_{44}) oscillators with subsequent phase modulation of this fluorescence by optically active molecules (θ) and birefringent networks (δ) of such molecules. In this case, the information content of the matrix elements is different. Thus, the set of elements $M_{i=1;k=1,2,3,4}(F_{12})$ characterises the fluorescence of linear oscillators, which arose due to the optically anisotropic absorption. Elements $M_{i=2,3;k=1,2,3,4}(F_{21,22,33})$ determine the phase-modulated (δ,θ) fluorescence of linear oscillators. Finally, the elements $M_{i=4;k=1,2,3,4}(F_{21,22,33}, F_{44})$ yield comprehensive information about the fluorescence of linear ($F_{21,22,33}$) and elliptic (F_{44}) oscillators in an optically anisotropic medium with linear and circular birefringence.

Note that the practical use of expression (8) presents some difficulties. The reason for this fact is the azimuth dependence of the majority of the matrix components – in the general case, 12 elements out of 16 undergo changes when the sample is rotated around the probe axis. This problem can be solved by using the data of papers [7, 8]. Here we show that the azimuth stable (independent of the angle Θ of the sample rotation) are the following elements of the matrix $\{M\}$: M_{11}, M_{14}, M_{41}, and M_{44}.

Thus, having measured experimentally the coordinate distributions of the elements $q \equiv \{M_{14,41}\}$ in the given spectral range $\lambda = 0.63-0.65$ μm using a digital camera, we can obtain the azimuth-stable information about the fluorescence of porphyrins of optically anisotropic tissue structures in human organs.

3. Analysis and discussion of the experimental data

Two groups of optically thin (geometrical thickness, $l \approx 20$ μm; attenuation coefficient, $\tau \leqslant 0.1$) histological sections of biopsy of benign (polyp, group I consisting of 27 samples) and malignant (adenocarcinoma, group II consisting of 26 samples) tumours of rectal tissue served as the samples.

Experimental measurements were carried out for the standard position of the Stokes polarimeter [11–13] with the use of a spectrally selective 'cut-off' filter ($\lambda = 0.63$ μm), placed in front of the digital camera recording images of the experimental samples. For the autofluorescence to be excited, we used a solid-state 'blue' laser with a power of $W = 50$ μW and a wavelength of $\lambda = 0.412$ μm. The polarisation illuminator consisted of two quarter-wave plates and a polariser. The images of the samples were projected by a polarising microscope objective (Nikon CFI Achromat P, focal length of 30 mm, aperture of 0.1, a magnification of 4×) onto the photosensitive plane of the CCD-camera [The Imaging Source DMK 41AU02.AS, monochrome 1/2″ CCD, Sony ICX205AL (progressive scan); the resolution of 1280 × 960, the photosensitive area of 7600 × 6200 mm, the sensitivity of 0.05 lx, the 8-bit dynamic range, the SNR of 9 bits, the deviation from linear photosensitivity of no more than 15%]. The polarisation analysis of fluorescent images of the samples was carried out using the quarter-wave plate and a polariser-analyser. Using the data obtained, we calculated the array $(m \times n)$ of the quantities

$$M_{14} = S_1^{\otimes} - 0.5(S_1^0 + S_1^{90}),$$
$$M_{41} = 0.5(S_0^4 + S_4^{90}). \tag{9}$$

Here, $S_{i=1,4}^{0,90,\otimes}$ are the parameters of the Stokes vector at the points of the digital image of the histological section, measured for a series of linearly (0°, 90°) and right-hand (⊗) polarised probe laser beams.

Objective evaluation of the coordinate distributions of $q(m \times n)$ was performed within the framework of the statistical approach. We calculated a set Z_i of statistical moments of the 1st-to-4th orders:

$$Z_1 = \frac{1}{P}\sum_{j=1}^{P}|q|, \quad Z_2 = \sqrt{\frac{1}{P}\sum_{j=1}^{P}(q_j - Z_1)^2}, \tag{10}$$

$$Z_3 = \frac{1}{Z_2^3}\frac{1}{P}\sum_{j=1}^{P}q^3, \quad Z_4 = \frac{1}{Z_2^4}\frac{1}{P}\sum_{j=1}^{P}q^4,$$

where $P = m \times n$ is the number of the CCD-camera pixels.

Figures 1 and 2 shows the results of Mueller-matrix mapping of laser autofluorescence of the ensembles of linear (M_{14}, Fig. 1) and elliptic (M_{41}, Fig. 2) oscillators – liquid crystal molecules and chains of porphyrins of histological sections of biopsy of benign and malignant tumours.

Analysis of the coordinate distributions of the invariant M_{14} (Figs 1a and 1b), which characterises the process of conversion of the circularly polarised fluorescence into the linearly polarised one, demonstrates the displacement of the main extremum of the histogram $N(M_{14})$ to lower values ($M_{14}\downarrow$) of this parameter in the plane of the histological section of adenocarcinoma tissue (Figs 1c and 1d). An opposite situation is observed for the distributions of the Mueller-matrix invariant (Figs 2a and 2b), which characterises the process of conversion of the linearly polarised fluorescence into the circularly polarised one. The histological section of the malignant tumour demonstrates an increase in the probability of extreme values, $M_{41} \to 1$ (Fig. 2d).

Let us analyse the obtained results from the physical point of view. Within the framework of the model considered here, the fluorescence of porphyrins is characterised by a set of 'linear' [$F_{12,21,22,33}(a,b)$] and 'elliptic' [$F_{44}(c)$] oscillators. These emitters are located in an optically anisotropic matrix with linear (6) and circular (7) birefringence. It is known [11–14] that the orientation-phase (δ,θ) structure of such a matrix depends on the pathology of biological tissue. Thus, malignant pathologies are characterised by a direction- ($\Delta\rho\uparrow$) and birefringence-disordered ($\Delta n\uparrow$) fibrillar network. On the other hand, the authors of [23, 26–28] showed that the autofluorescence in the red region of the spectrum increases with progression and growth of neoplastic lesions. This phenomenon may be due to the liquid crystal networks of porphyrins accumulated in tissues of malignant tumours at different stages of their growth. Therefore, malignant pathologies are accompanied by the formation of a system of 'elliptic' fluorescent emitters

$$a\downarrow, b\downarrow \to F_{12,21,22,33}(a,b)\downarrow,$$

$$c\uparrow \to F_{44}(c)\uparrow,$$

which prevail over disordered 'linear' oscillators.

On the contrary, the precancerous condition is characterised by the predominance of a more orderly system of 'linear' fluorescent emitters,

$$a\uparrow, b\uparrow \to F_{12,21,22,33}(a,b)\uparrow,$$

$$c\downarrow \to F_{44}(c)\downarrow.$$

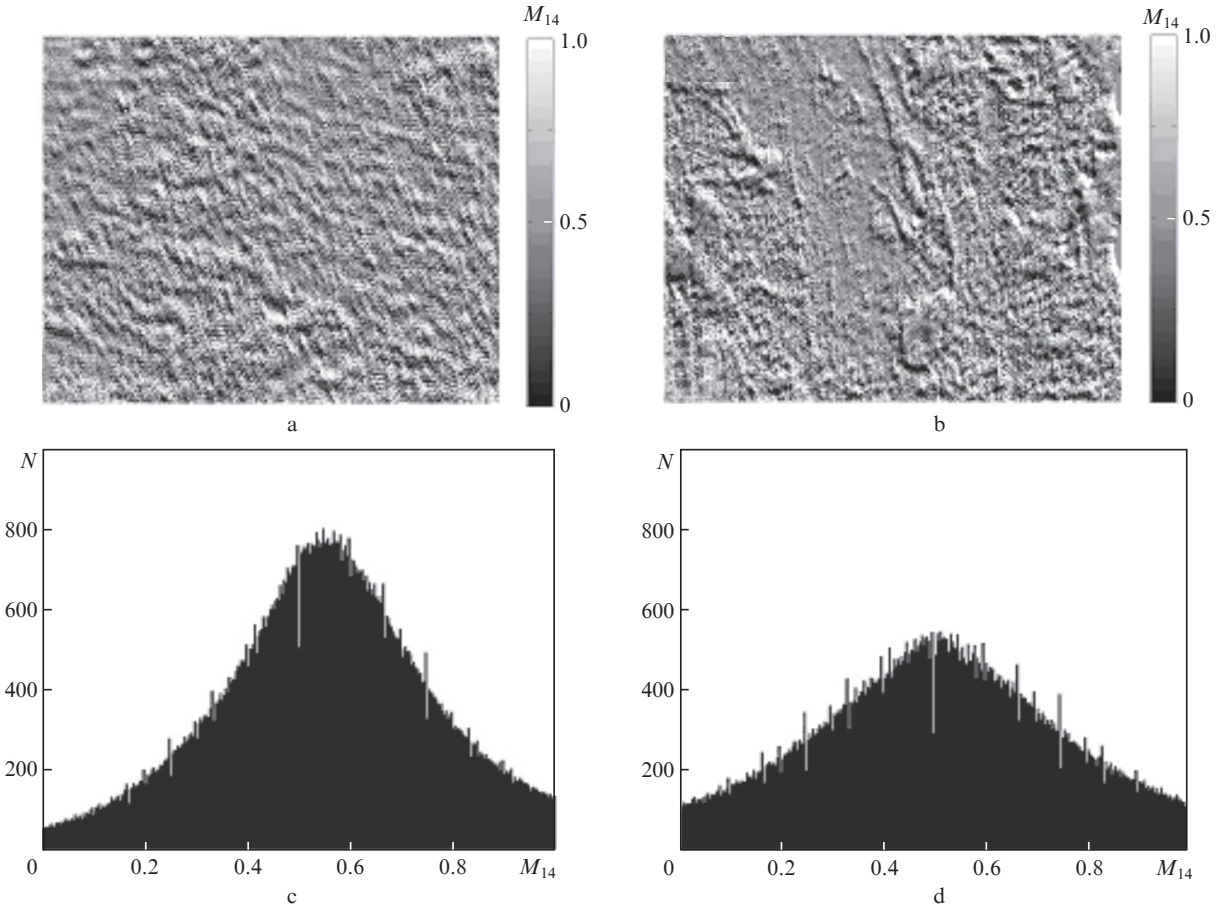

Figure 1. (a, b) Coordinate distributions of M_{14} and (c, d) histograms $N(M_{14})$ of histological sections of (a, c) polyp and (b, d) adenocarcinoma of the rectum.

The secondary phase modulation of the fluorescence by fibrillar networks of both types of samples manifests itself in opposite changes in the Mueller-matrix invariants M_{14} and M_{41}. Because the 'cancerous' condition is characterised by an increase in birefringence ($\Delta n\uparrow$) of protein structures, $M_{41}\uparrow$. In other words, for malignant neoplasms the following analytical scenario

$$a\downarrow, b\downarrow \rightarrow F_{12,21,22,33}(a,b)\downarrow \Rightarrow M_{14}\Downarrow,$$

$$c\uparrow \rightarrow F_{44}(c)\uparrow \Rightarrow M_{41}\Uparrow$$

is realised.

For tissue with dysplasia the inverse holds true:

$$a\uparrow, b\uparrow \rightarrow F_{12,21,22,33}(a,b)\uparrow \Rightarrow M_{14}\Uparrow,$$

$$c\downarrow \rightarrow F_{44}(c)\downarrow \Rightarrow M_{41}\Downarrow.$$

To identify a possible clinical use of laser fluorescence polarimetry we conducted its comparative tests with the method of direct Mueller-matrix mapping. To this end, within the two statistically significant groups (confidence interval $p < 0.001$) of the samples we determined:

(i) average values and standard deviations of the statistical moments $Z_{i=1,2,3,4}(q)$ (Tables 1 and 3);

(ii) operating characteristics traditional for evidence based medicine, i.e., sensitivity $\{\mathrm{Se} = [a/(a+b)] \times 100\%\}$, specificity $\{\mathrm{Sp} = [c/(c+d)] \times 100\%\}$ and accuracy [Ac = (Se + Sp)/2], where a and b are the number of correct and incorrect diagnoses within group I; and c and d are the number of correct and incorrect diagnoses within group II (Tables 2 and 4).

Table 1. Statistical moments of the 1st-to-4th orders of distributions of Mueller-matrix invariants M_{14} and M_{41} (laser polarimetry).

Z_i	M_{14}		M_{41}	
	Group I	Group II	Group I	Group II
Z_1	0.11 ± 0.018	0.86 ± 0.11	0.14 ± 0.024	0.11 ± 0.016
Z_2	0.08 ± 0.011	0.26 ± 0.038	0.11 ± 0.019	0.09 ± 0.012
Z_3	0.92 ± 0.11	0.61 ± 0.078	0.53 ± 0.082	0.79 ± 0.13
Z_4	0.39 ± 0.23	1.87 ± 0.22	1.04 ± 0.16	0.55 ± 0.22

Table 2. Operating characteristics of the methods of direct Mueller-matrix mapping.

Z_i	M_{14}			M_{41}		
	Se (%)	Sp (%)	Ac (%)	Se (%)	Sp (%)	Ac (%)
Z_1	58	52	55	64	52	53
Z_2	56	52	54	62	50	56
Z_3	62	54	58	68	60	64
Z_4	64	54	59	70	60	65

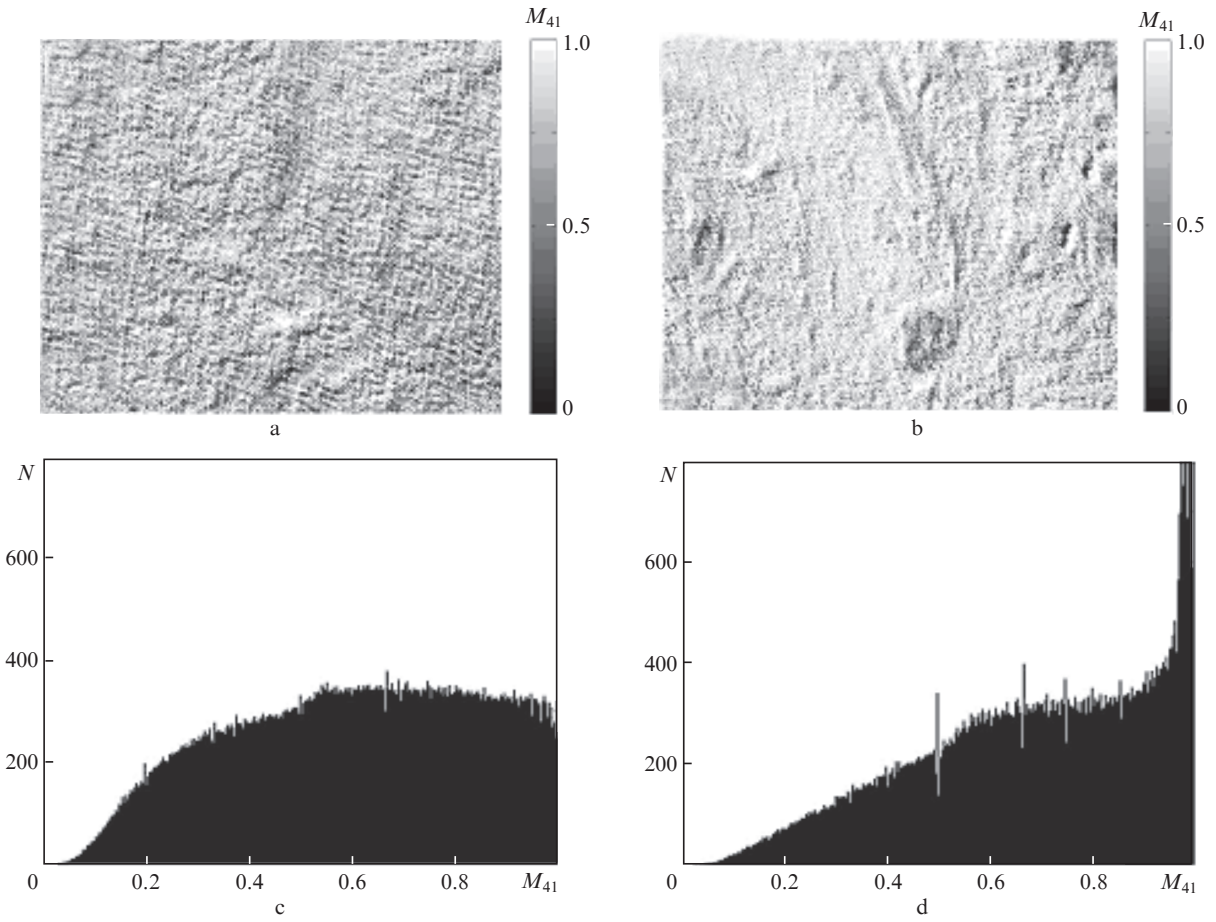

Figure 2. (a, b) Coordinate distributions of M_{41} and (c, d) histograms $N(M_{41})$ of histological sections of (a, c) polyp and (b, d) adenocarcinoma of the rectum.

Table 3. Statistical moments of the 1st-to-4th orders of distributions of Mueller-matrix invariants M_{14} and M_{41} (laser autofluorescence polarimetry).

Z_i	$M_{14}(\lambda_f)$		$M_{41}(\lambda_f)$	
	Group I	Group II	Group I	Group II
Z_1	0.63 ± 0.088	0.49 ± 0.061	0.68 ± 0.096	0.89 ± 0.12
Z_2	0.14 ± 0.022	0.18 ± 0.023	0.27 ± 0.039	0.16 ± 0.023
Z_3	0.33 ± 0.045	0.21 ± 0.032	0.81 ± 0.12	1.69 ± 0.19
Z_4	0.49 ± 0.057	0.28 ± 0.035	0.67 ± 0.11	1.95 ± 0.26

Table 4. Operating characteristics of the method of Mueller-matrix fluorescent mapping.

Z_i	$M_{14}(\lambda_f)$			$M_{41}(\lambda_f)$		
	Se (%)	Sp (%)	Ac (%)	Se (%)	Sp (%)	Ac (%)
Z_1	66	58	62	68	60	64
Z_2	68	54	61	72	62	67
Z_3	74	66	70	92	78	85
Z_4	82	70	76	94	82	88

Analysis of the data shows the highest sensitivity of the statistical moments of the 3rd and 4th orders, characterising the distribution of $M_{41}(m \times n)$, to the type of pathology of rectal tissue. In this case, the differences between their values reach about 50%. From a physical point of view, the results can be attributed to a greater phase modulation of laser emission by a birefringent network of the histological section of adenocarcinoma. However, the specificity Sp and accuracy Ac of the method of direct Mueller-matrix mapping of histological sections of the polyp and adenocarcinoma are not high enough, i.e., do not exceed 60%–65% (Table 2).

For the statistical moments $Z_{i=1,2,3,4}(q)$, which characterise the distributions of $M_{14}(\lambda_f)$ and $M_{41}(\lambda_f)$, we found the following ranges of intergroup differences:

$$M_{14}(\lambda_f)\text{: } \Delta Z_1 \leftrightarrow 1.28,\ \Delta Z_2 \leftrightarrow 1.28,\ \Delta Z_3 \leftrightarrow 1.57,\ \Delta Z_4 \leftrightarrow 1.75;\text{'}$$

$$M_{41}(\lambda_f)\text{: } \Delta Z_1 \leftrightarrow 1.3,\ \Delta Z_2 \leftrightarrow 1.69,\ \Delta Z_3 \leftrightarrow 2.08,\ \Delta Z_4 \leftrightarrow 2.91.$$

It can be seen that the intergroup differences between the statistical moments $Z_{i=1,2,3,4}(M_{41})$ are much greater than in the case of the method of direct polarisation mapping. These results can be attributed to the model analysis [relations (1)–(8)] of the porphyrin fluorescence. According to the approach discussed, the cancer pathology is characterised by the formation of a system of 'elliptic' fluorescent emitters ($F_{44}\uparrow$) and by an increase in the birefringence of the fibrillar network of adenocarcinoma ($M_{41}\uparrow$). Therefore, the main extremum of the histogram $N(M_{41})$ is shifted ($M_{41} \to 1$). As a result, the average ($Z_1\uparrow$), asymmetry ($Z_3\uparrow$) and sharpness of the peak ($Z_4\uparrow$) of the distribution significantly increase and hence the range of intergroup differences between the sets of statistical moments grows. This is the basis for increasing the

informativeness of the Mueller-matrix fluorescence mapping (Table 4).

Thus, the spectrally selective Mueller-matrix mapping of the porphyrin fluorescence proved to be effective in the differential diagnosis of benign (polyp) and malignant (adenocarcinoma) tissues of the rectum – M_{14} (Ac = 70%–76%) and M_{41} (Ac = 85%–88%).

4. Conclusions

Using the generalised Mueller-matrix model of the fluorescence of birefringent networks of optically active complexes of biological tissues we have developed a method of spectrally selective autofluorescence polarimetry.

We have determined the Mueller-matrix azimuth-stable invariants of laser autofluorescence characterising polarisation manifestations of the porphyrin fluorescence against the background of linear birefringence and optical activity of proteins of biological tissues.

Within the framework of the statistical approach, we have performed a comparative study of diagnostic possibilities of the methods of direct Mueller-matrix mapping and laser autofluorescence polarimetry of rectal tissue with benign (polyp) and malignant (adenocarcinoma) pathologies.

We have demonstrated the clinical efficacy of the statistical analysis of the coordinate distributions of Mueller-matrix invariants of laser polarisation autofluorescence as applied to the problem of differentiation of benign and malignant tumours of rectal tissue.

References

1. Bueno J.M., Jaronski J. *Ophthal. Physiol. Opt*., **21**, 384 (2001).
2. Bueno J.M., Vargas-Martin F. *Appl. Opt*., **41**, 116 (2002).
3. Bueno J.M., Campbell M.C.W. *Ophthal. Physiol. Opt*., **23**, 109 (2003).
4. Tower T.T. *Biophys. J*., **81**, 2954 (2001).
5. Tower T.T., Tranquillo R.T. *Biophys. J*., **81**, 2964 (2001).
6. Shribak M., Oldenbourg R. *Appl. Opt*., **42**, 3009 (2003).
7. Smith M.H., Burke P., Lompado A., Tanner E., Hillman L.W. *Proc. SPIE Int. Soc. Opt. Eng*., **3991**, 210 (2000).
8. Smith M.H. *Proc. SPIE Int. Soc. Opt. Eng*., **4257**, 82 (2001).
9. Wang X., Wang L.V. *J. Biomed. Opt*., **7**, 279 (2002).
10. Lu S., Chipman R.A. *J. Opt. Soc. Am. A*, **13**, 1106 (1996).
11. Ushenko A.G., Pishak V.P. *Handbook of Coherent-Domain Optical Methods: Biomedical Diagnostics, Environmental and Material Science*. Ed. by V.V. Tuchin (Boston: Kluwer Acad. Publ., 2004) Vol. 1, pp 93–138.
12. Angelsky O.V., Pishak V.P., Ushenko A.G., Ushenko Yu.A., in *Optical Correlation Techniques and Applications*. Ed. by O.V. Angelsky (Bellingham: SPIE Press, 2007) pp 213–266.
13. Angelsky O.V., Ushenko A.G., Ushenko Yu.A., Pishak V.P., Peresunko A.P., in *Handbook of Photonics for Biomedical Science*. Ed. by V.V. Tuchin (Boca Raton–London–New York: CRC Press, Taylor&Francis group, 2010) pp 283–322.
14. Andersson-Engels S., Klinteberg C., Svanberg K., Svanberg S. *Phys. Med. Biol*., **42**, 815 (1997).
15. Alfano R.R., Das B.B., Cleary J., et al. *Bull. NY Acad. Med*., **67**, 143 (1991).
16. Anidjar M., Ettori D., Cussenot O., et al. *J. Urol*., **156**, 1590 (1996).
17. Bohorfoush A.G. *Endoscopy*, **28**, 372 (1996).
18. Chwirot B., Jedrzejczyk W., Chwirot S., et al. *Pol. Merkuriusz. Lek*., **5**, 355 (1996).
19. Bard M., Amelink A., Skurichina M., et al. *Chest*, **129**, 995 (2006).
20. Beamis J., Ernst A., Mathur P., et al. *Lung Cancer*, **41**, 49 (2003).
21. Snindo Y., Oda Y. *Appl. Spectrosc*., **46**, 1251 (1992).
22. Arteaga O., Nicols S., Kahr B. *Opt. Lett*., **37**, 2835 (2012).
23. Alfano R.R., Tata D.B., Tomashefsky P., et al. *IEEE J. Quantum Electron*., **20**, 1502 (1984).
24. Savenkov S.N., Marienko V.V., Oberemok E.A., Sydoruk O.I. *Phys. Rev. E*, **74**, 605 (2006).
25. Zellweger M. *Fluorescence Spectroscopy of Exogenous, Exogenously-induced and Endogenous Fluorofores for the Photodetection and Photodynamic Therapy of Cancer* (Lausanne: Fevrier, 2000).
26. Stroka R., Baumgartner R., Buser A. et al. *Proc. SPIE Int. Soc. Opt. Eng*., **1641**, 99 (1991).
27. D'Hallewin M., Kamuhabvra A., Roskams T., et al. *BJU Int*., **89**, 760 (2002).
28. D'Hallewin M.A., Bezdetnaya L., Guillemin F. *Eur. Urol*., **42**, 417 (2002).